where $\hat{\mathbf{d}}_i$ is the dipole operator of atom i, $\mathbf{e}_{r_{ij}}$ is the unit vector connecting the two atoms, and r_{ij} their distance. Mapped Eq. (A3) on the spin Hamiltonian of Eq. (1), the resulting interaction coefficient is

$$J_{ij}^{\perp} = \frac{C_3^{\perp}(1 - 3\cos^2\theta_{\mathrm{ij}})}{r_{ij}^3}. \tag{A4}$$

Here, θ_{ij} is the angle between $\mathbf{e}_{r_{ij}}$ and the quantization axis and $C_3^{\perp}$ the coupling parameter [36,37]. The Ising term $J_{ij}^{\parallel}$ is zero since interaction energy shifts $E_{\alpha_i\beta_j}$ are dipole forbidden. Therefore, this is a way to realize an XX model as depicted in Fig. 1(b). In this paper, we have chosen $|61S\rangle$ and $|61P\rangle$ leading to $C_3^{\perp}/2\pi = 3.14\,\mathrm{GHz\mu m^3}$.

In the case where the two chosen states possess the same parity, such as the two atoms being in the same state $|nS\rangle$, direct dipolar coupling is forbidden and the leading interaction is a second-order process through a virtually excited pair state $|m\rangle$ and can be described by

$$\hat{H}_{vdW} = -\frac{1}{\hbar}\sum_m \frac{\hat{H}_{\mathrm{DDI}}|m\rangle\langle m|\hat{H}_{\mathrm{DDI}}}{\Delta_v}. \tag{A5}$$

Here, the Foerster defect Δ_v is the energy difference between the initial state and the virtually excited state $|m\rangle$. This Hamiltonian gives rise to power-law interactions $J_{ij} = C_6/r_{ij}^6$ that scales with n^{11}. Especially, this term is large if a pair state $|m\rangle$ with a small Foerster defect exists. Many experiments exploit these interactions to realize a spin system where the ground state is coupled to a single Rydberg state. These systems feature the Rydberg blockade effect and can be mapped on an Ising model [3,34,35].

Similar interactions also exist for a spin system realized with two different Rydberg states $|\downarrow\rangle = |nS\rangle$ and $|\uparrow\rangle = |(n+1)S\rangle$. In this case, the van der Waals Hamiltonian (A5) also induces a spin exchange term because the two Rydberg states are coupled via the intermediate pair state $|m\rangle = |nP, nP\rangle$ [see Fig. 1(c)]. In the case of $n = 61$, both the Ising and exchange interactions terms are similar with $J^{\parallel}/J^{\perp} = -0.7$. Therefore, this spin system can be mapped onto an effective Heisenberg XXZ-Hamiltonian [21].

In order to realize an Ising Hamiltonian with two different Rydberg states, a state combination is needed where the exchange term (A2) is small requiring a large Foerster defect Δ_v [see Fig. 1(d)]. This can be achieved by coupling $|\downarrow\rangle = |nS\rangle$ to $|\uparrow\rangle = |(n+3)S\rangle$. In this case, the largest contribution to the exchange term comes from $|m\rangle = |(n+1)P, (n+1)P\rangle$. For example, for $n = 61$, this spin system is characterized by a ratio of $J^{\parallel}/J^{\perp} = 400$, which is a good approximation to an Ising Hamiltonian ($J^{\perp} = 0$).

TABLE I. Waists of the blue (480 nm) and red (780 nm) Rydberg excitation lasers used to realize the different models and the respective ground state cloud waists.

Model	blue exc. $\sigma_{x,y}$	red exc. $\sigma_{x,y}$	GS σ_x	GS $\sigma_{y,z}$
Ising	55 µm	1.5mm	64 µm	45 µm
XXZ	55 µm	1.5mm	64 µm	45 µm
XX	55 µm	1.5mm	62 µm	47 µm

APPENDIX B: EXPERIMENTAL IMPLEMENTATION OF VARIOUS SPIN MODELS

To realize the Heisenberg XX model, a single-photon microwave transition at $2\pi \times 16\,\mathrm{GHz}$ with a Rabi frequency of $\Omega = 2\pi \times 18\,\mathrm{MHz}$ couples the state $|\downarrow\rangle$ to $|\uparrow\rangle = |61P_{3/2}, m_j = 1/2\rangle$. To implement the XXZ Hamiltonian,

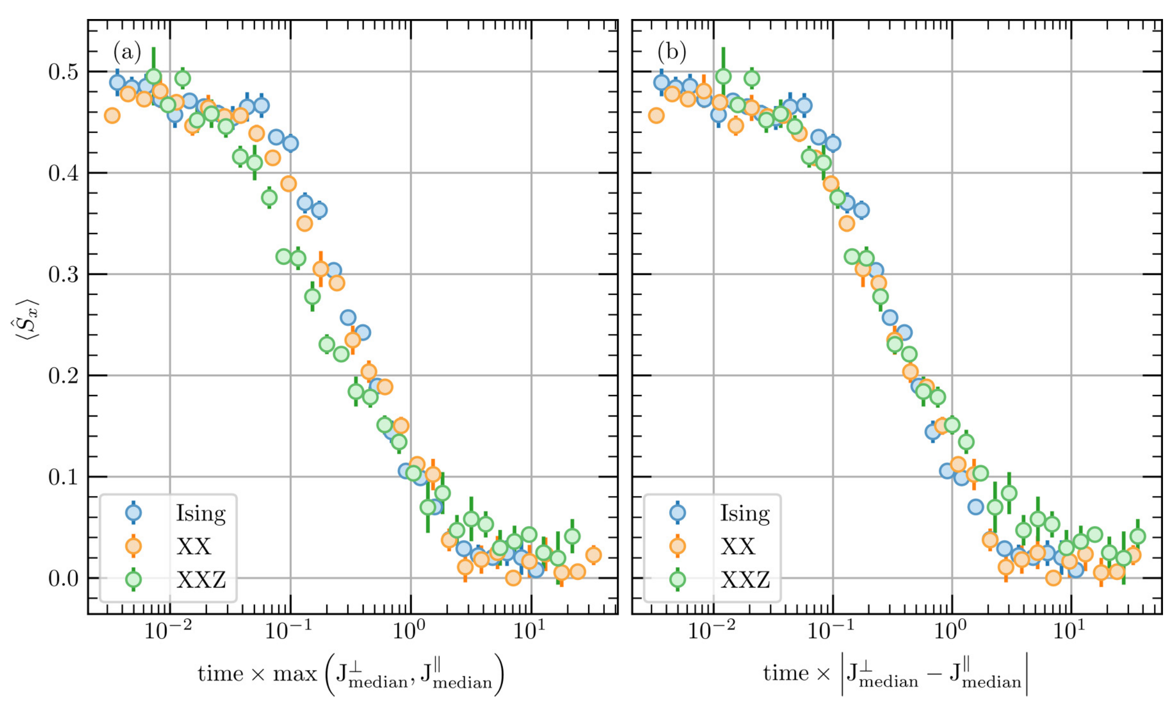

FIG. 5. Comparison of the scaling behavior for rescaling time either by the median interaction matrix (a) or by the median of the pair oscillation frequency (b). max($J^{\perp}_{\mathrm{median}}, J^{\parallel}_{\mathrm{median}}$) is defined as $J^{\perp}_{\mathrm{median}}$ for the Heisenberg XX and XXZ model, and as $J^{\perp}_{\mathrm{median}}$ for the Ising model.